The Journal of Immunology

Sialylation of N-Linked Glycans Influences the Immunomodulatory Effects of IgM on T Cells

Manuela Colucci, Henning Stockmann, Alessia Butera, Andrea Masotti, Antonella Baldassarre, Ezio Giorda, Stefania Petrini, Pauline M. Rudd, Roberto Sitia, Francesco Emma and Marina Vivarelli

J Immunol published online 24 November 2014
http://www.jimmunol.org/content/early/2014/11/23/jimmunol.1402025

The Journal of Immunology is published twice each month by The American Association of Immunologists, Inc., 1451 Rockville Pike, Suite 650, Rockville, MD 20852

Print ISSN: 0022-1767 Online ISSN: 1550-6606.

Published November 24, 2014, doi:10.4049/jimmunol.1402025

Sialylation of N-Linked Glycans Influences the Immunomodulatory Effects of IgM on T Cells

Manuela Colucci,* Henning Stockmann,† Alessia Butera,* Andrea Masotti,‡ Antonella Baldassarre,‡ Ezio Giorda,§ Stefania Petrini,¶ Pauline M. Rudd,† Roberto Sitia,‖ Francesco Emma,* and Marina Vivarelli*

Human serum IgM Abs are composed of heavily glycosylated polymers with five glycosylation sites on the μ (heavy) chain and one glycosylation site on the J chain. In contrast to IgG glycans, which are vital for a number of biological functions, virtually nothing is known about structure–function relationships of IgM glycans. Natural IgM is the earliest Ig produced and recognizes multiple Ags with low affinity, whereas immune IgM is induced by Ag exposure and is characterized by a higher Ag specificity. Natural anti-lymphocyte IgM is present in the serum of healthy individuals and increases in inflammatory conditions. It is able to inhibit T cell activation, but the underlying molecular mechanism is not understood. In this study, to our knowledge, we show for the first time that sialylated N-linked glycans induce the internalization of IgM by T cells, which in turn causes severe inhibition of T cell responses. The absence of sialic acid residues abolishes these inhibitory activities, showing a key role of sialylated N-glycans in inducing the IgM-mediated immune suppression. ***The Journal of Immunology*****, 2015, 194: 000–000.**

Natural IgM, the first line of defense in humoral immune responses, is capable of reacting with multiple ligands with low affinity. Following Ag stimulation, instead, specific immune IgM are produced with higher affinity (1). Serum IgM are polymers with a predominantly pentameric structure, consisting of $(\mu_2L_2)_5$ polymers, generally joined by a J chain. However, circulating hexameric IgM, lacking the J chain, can also be found (2, 3). This polymeric structure with multiple binding sites determines a high avidity that compensates the low affinity of the natural IgM (3). IgM are highly glycosylated, with five N-glycans attached to μ (heavy) chain and one present on the J chain. This makes polymeric IgM bound to apoptotic cells and bacteria efficient activators of complement, and their N-glycan moieties bind mannose-binding lectin, leading to cell lysis (4). Natural anti-lymphocyte IgM have been identified in the serum of healthy individuals. Their levels increase in different inflammatory conditions and diseases such as HIV infections, end-stage renal disease, and systemic lupus erythematosus (5–7). When purified, these IgM can exert inhibitory effects on anti-CD3–induced T cell activation, or chemotaxis, in response to CXCL12 and CCL3 (8, 9). This effect is protective in inflammatory conditions and allograft rejection and prevents the development of autoimmune diabetes (8–12). However, the mechanisms underlying the inhibitory effects of natural anti-lymphocyte IgM are still unclear. Previous studies on IgG revealed an anti-inflammatory role for terminal sialylation of the N-glycans present on the γ-chain (13). In this study, we investigated whether and how the processing of N-glycans, and in particular the presence or absence of terminal sialic acid residues, influences the immunomodulatory effects of IgM on T cells. Our findings reveal a key role of sialylated N-glycans in IgM–T cell interactions.

Materials and Methods

Abs

Human IgM purified from serum of healthy donors (IgMh) was from Sigma-Aldrich (IgMh1) and A50168H was from Meridian Life Science (IgMh2). Human IgM purified from myeloma serum (IgMm) was provided by Jackson Lab ImmunoResearch (IgMm1); A32169H was from Meridian Life Science (IgMm2); and OBT1524 was from AbDSerotec (IgMm3). Fluorochrome-conjugated Abs Alexa Fluor 700 and FITC anti-CD3, allophycocyanin anti-CD4, PE anti-CD8, and Cychrome anti-CD19 were from BD Biosciences, and Alexa Fluor 647 anti-IgM was from Jackson ImmunoResearch Laboratories. Mouse anti-human IgM mAb was provided by Invitrogen; HRP-conjugated goat anti-mouse Ab was provided by Santa Cruz; and mouse anti-human J chain Ab was provided by Serotec. Mouse anti-human LAMP-1 Ab was from Santa Cruz, and goat anti-mouse Alexa 555 Ab was from Invitrogen.

Reagents

Dynabeads Human T-Activator CD3/CD28 was from Life Technologies; bafilomycin A1 (BFM) was from Sigma-Aldrich; trypsin-EDTA was from Euroclone; PHA was from Sigma-Aldrich; 5-chloromethylfluorescein diacetate (CMFDA; CellTracker) was from Molecular Probes; fetuin was from Sigma-Aldrich; and Alexa 568 transferrin was from Molecular Probes. Alexa Fluor 488–conjugated wheat germ agglutinin was provided by Molecular Probes; Hoechst 33342 was provided by Molecular Probes. α2-3,6,8,9 Neuraminidase A (catalogue P0722; preproduction lot) was provided by New England Biolabs. Triton X-100 was obtained from Sigma-Aldrich; paraformaldehyde was obtained from Sigma-Aldrich; and BSA fraction V was obtained from BDH.

*Division of Nephrology and Dialysis, Bambino Gesù Children's Hospital-Scientific Institute, 00165 Rome, Italy; †GlycoScience Group, National Institute for Bioprocessing Research and Training, Dublin, Ireland; ‡Gene Expression-Microarrays Laboratory, Bambino Gesù Children's Hospital-Scientific Institute, 00165 Rome, Italy; §Research Center, Bambino Gesù Children's Hospital-Scientific Institute, 00165 Rome, Italy; ¶Confocal Microscopy Core Facility, Research Center, Bambino Gesù Children's Hospital-Scientific Institute, 00165 Rome, Italy; and ‖Division of Genetics and Cell Biology, San Raffaele Scientific Institute, Università Vita-Salute San Raffaele, 20132 Milan, Italy

Received for publication August 18, 2014. Accepted for publication October 27, 2014.

This work was supported by the Associazione per la Cura del Bambino Nefropatico (to M.C.); European Union Seventh Framework Programme HighGlycan Grant 278535 (to H.S.); and Telethon and Associazione Italiana per la Ricerca sul Cancro (to R.S.).

Address correspondence and reprint requests to Dr. Marina Vivarelli, Division of Nephrology and Dialysis, Bambino Gesù Children's Hospital-Scientific Institute, Piazza S. Onofrio 4, 00165 Rome, Italy. E-mail address: marina.vivarelli@opbg.net

Abbreviations used in this article: BFM, bafilomycin A1; CMFDA, 5-chloromethylfluorescein diacetate; HILIC-UPLC-FLD, ultra-performance hydrophilic interaction liquid chromatography with fluorescence detection; IgMh, human IgM purified from serum of healthy donors; IgMm, human IgM purified from myeloma serum; IVIg, i.v. γ globulin; pIgR, polymeric IgR.

Cell collection and culture medium

Buffy coats collected from adult healthy donors were obtained from the Bambino Gesù Children's Hospital (Rome, Italy). Human PBMCs were isolated by Ficoll-Hypaque (Lympholyte M; Cedarlane Laboratories) density-gradient centrifugation. Informed consensus was obtained from all donors according to our Institutional Review Board guidelines and in compliance with the Declaration of Helsinki.

To discriminate T cells from other lymphoid cells, PBMCs were stained with fluorochrome-conjugated mAbs to CD3, CD19, and IgM, and gated CD3-positive and CD19-negative lymphocytes were analyzed by flow cytometry (FACSCanto II; BD Biosciences) using the FACSDiva software. Gated events (10,000) on living lymphocytes were analyzed for each sample.

In some experiments, T cells were isolated from PBMCs by cell sorting (FACSAria II; BD Biosciences) after staining with FITC anti-CD3, allophycocyanin anti-CD4, and PE anti-CD8 mAbs. Cells resulted in ≥99% CD3 positive, ≥99% CD4 positive, or ≥99% CD8 positive, as appropriate.

For all cell cultures, cells were incubated in RPMI 1640 (Life Technologies), supplemented with 10% FBS (Life Technologies), 1% L-glutamine (Life Technologies), and 1% penicillin/streptomycin (Euroclone) (defined as complete medium).

IgM binding and internalization assays

To analyze the ability of IgM to bind T cell surface, we cultured 2×10^5 PBMCs from healthy controls for 24 h at 37˚C with 25 μg/ml IgM purified from different human serum of healthy (IgMh) or myeloma (IgMm) donors. At the end of culture experiments, the IgM binding was measured by flow cytometry after staining with fluorochrome-conjugated anti-CD3, anti-CD19, and anti-IgM Abs, as previously described, and expressed as IgM mean fluorescence intensity. To define the basal level of IgM mean fluorescence intensity, cells were incubated with complete medium alone.

To characterize the IgM internalization, sorted T cells were incubated with IgMh1 or IgMm1, and lysosomal degradation was blocked by adding 50 nM BFM during incubation to permit intracellular accumulation of IgM. Cells were then washed and treated with 50 μg trypsin for 30 min at 37˚C to remove surface IgM, or incubated without trypsin to permit IgM internalization, with concomitant BFM treatment to maintain lysosomal blocking. At the end of the treatment, cells were washed and analyzed for the presence of IgM.

In some experiments, cells were collected to perform immunofluorescence analysis (see below).

All the experiments were performed in duplicate.

T cell activation and proliferation assays

PBMCs or sorted CD3-positive, CD4-positive, or CD8-positive T cells from healthy controls were labeled with 0.1 μg/ml CMFDA; cultured at 2×10^5 cells/well; stimulated by anti-CD3/anti-CD28 magnetic beads (bead-to-cell ratio = 1:3) or PHA (5 μg/ml); and incubated at 37˚C with native or desialylated IgM, fetuin, or transferrin (25 μg/ml). At day 1–4, cells were stained with fluorescent Abs to CD3 and CD19, and T cell proliferation was measured by FACS analysis.

In some experiments, CMFDA-labeled sorted T cells were incubated for 72 h with 25 μg/ml IgMh1 or IgMm1, and stimulated or not by anti-CD3/anti-CD28. Cell proliferation was then determined by FACS analysis, and RNA was extracted to analyze the expression of different activation genes by low-density gene expression arrays (see below).

Quantitative PCR expression analysis of immunity genes by low-density arrays

Total RNA was extracted by sorted T cells incubated or not incubated with IgMh1 and IgMm1 and activated by anti-CD3/anti-CD28 stimulation for 72 h, using the total RNA extraction kit (Norgen). An amount of 1 μg total RNA was reverse transcribed using the High Capacity cDNA Archive kit (Life Technologies), according to the manufacturer's instructions. An amount of 100 ng cDNA (in 50 μl) was mixed with Universal PCR Master Mix (Life Technologies) in a final volume of 100 μl and loaded into the microfluidic card (TaqMan Human Immune Array). Gene expression levels were determined by considering β-glucuronidase as the endogenous control gene and applying the ΔΔ cycle threshold method for relative quantity calculation (14).

Western blot

For the characterization of purified IgM, proteins were separated onto a 10% reducing SDS-PAGE gel, or a precast 4–15% gradient gel (Bio-Rad) in nonreducing conditions, and blots were decorated for 1 h with monoclonal mouse anti-human IgM (1 μg/ml in TBST) or anti-J chain (5 μg/ml in TBST), followed by HRP-conjugated goat anti-mouse Ab (0.1 μg/ml in TBST). Between the incubations, membranes were washed three times in TBST for 10 min.

Immunofluorescence analysis

Sorted T cells incubated for 24 h at 37˚C with 25 μg/ml IgMh1 or IgMm1 were fixed at room temperature for 10 min in 4% paraformaldehyde, spotted onto poly-L-lysine–coated glass slides (Thermo Scientific), and allowed to adhere for 30 min at 37˚C. Cells were permeabilized for 10 min in 0.1% Triton X-100 and blocked for 30 min in PBS with 5% BSA. Cells were then stained for 1 h at room temperature with 10 μg/ml Alexa Fluor 647 anti-IgM Ab, washed three times in PBS, and stained at room temperature for 20 min with 5 μg/ml 488-conjugated wheat germ agglutinin. After washing with PBS, cells were labeled with 1 μg/ml Hoechst for 5 min, and slides were mounted in 50% glycerol in PBS. Confocal images were acquired by Olympus Fluoview FV100 confocal microscope using an immersion oil 63× objective. Images were processed using Adobe Photoshop 9.0.

In some experiments, sorted T cells treated with 50 nM BFM during IgM incubation were subjected to trypsin digestion to remove surface IgM or incubated without trypsin to permit IgM internalization, as described below, before immunofluorescence analysis. Lysosomal localization was determined by staining with 1 μg/ml anti–LAMP-1 mAb, followed by incubation with 5 μg/ml Alexa 555 goat anti-mouse Ab.

Glycan analysis

Glycan sample preparation was performed, as described earlier (15), using 50–100 μg IgM per sample (buffered aqueous solution as supplied). Each IgM sample was reduced, alkylated, and deglycosylated. Glycans were labeled with 2-aminobezamide, and samples were cleaned up by solid-phase extraction and analyzed by ultra-performance hydrophilic interaction liquid chromatography with fluorescence detection (HILIC-UPLC-FLD) on a Waters Acquity UPLC H-Class instrument, as described earlier (15). A dextran hydrolysate ladder was used to convert retention times into glucose unit values. Data were processed by Waters Empower 3 chromatography workstation software. Gycans were represented using the Oxford symbol nomenclature (16).

To desialylate IgM, a solution of α2-3,6,8,9 neuraminidase A (400 U) was added to a solution of 300 μg IgMh1 (1 mg/ml buffered aqueous solution as supplied). The solution was incubated at 15˚C with agitation at 300 rpm for 12 h. The resulting product was affinity purified on a Hamilton Star liquid-handling workstation, which resulted in 80 μg desialylated IgM (27% yield). Finally, the elution buffer was exchanged into PBS by using an Amicon Ultra 100-kDa ultrafiltration device. The polymeric conformation of the desialylated IgM was confirmed by nonreducing SDS-PAGE, and the glycosylation profile was confirmed by HILIC-UPLC-FLD, as described above.

Statistical analysis

Statistical comparison between various groups was performed by Student *t* test or one-way ANOVA with either least significant difference or Bonferroni post hoc tests, as appropriate, using the SPSS software (12.0.2). Comparisons were made between means from several experiments. Differences were considered significant when p values <0.05.

Results

IgM detection on T cell surface reflects a different IgM internalization

To determine the ability of IgM to bind T cells, we incubated human PBMCs from healthy donors with five commercially available IgM formulations purified from the serum of human healthy donors (IgMh) or myeloma patients (IgMm) for 24 h at 37˚C. Only one myeloma IgM formulation (IgMm1) was strongly detected on the surface of T cells after incubation (Fig. 1A). Immunofluorescence analysis of sorted T cells incubated with IgM showed that, whereas IgMm1 remained on the cell surface, IgMh1 bound T cells and became internalized (Fig. 1B). To verify this internalization, we incubated sorted T cells with BFM during incubation with IgM, to block lysosomal degradation, and removed surface IgM by trypsin digestion. Immunofluorescence analysis demonstrated that only a fraction of IgMh1—but not of IgMm1—was resistant to trypsin digestion, confirming the internalization of

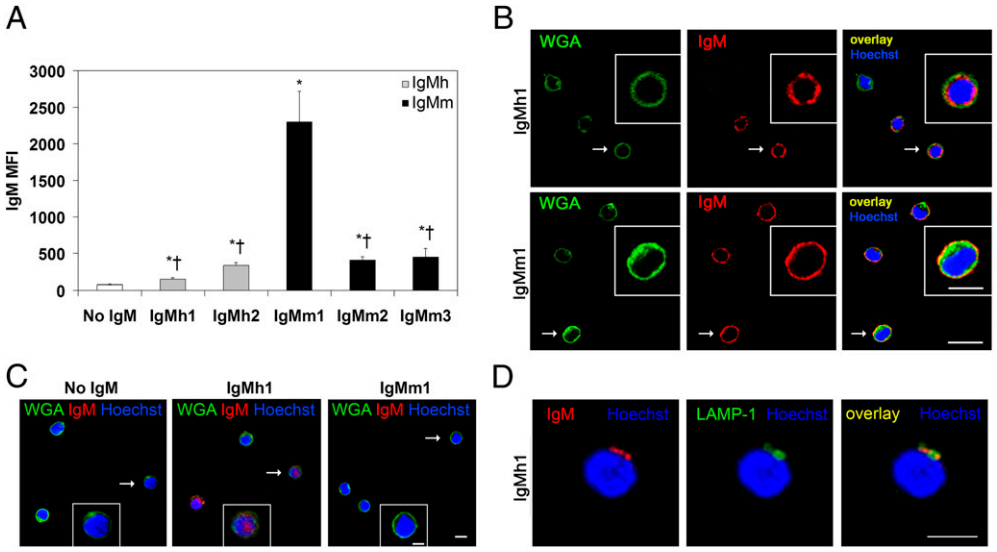

FIGURE 1. IgM detection on T cell surface reflects a different IgM internalization. (**A**) PBMCs were incubated with IgMh or IgMm for 24 h at 37°C and analyzed by FACS after staining with fluorescent Abs to CD3, CD19, and IgM. The mean fluorescence intensity (MFI) obtained by anti-IgM staining was compared on gated living T cells incubated with different IgM preparations. Data represent the mean ± SEM ($n = 4$). *$p < 0.02$ versus cells not incubated with IgM as determined by paired t test, †$p < 0.05$ versus the incubation with IgMm1. (**B**) Sorted T cells were incubated with IgMh1 or IgMm1 for 24 h at 37°C and analyzed by confocal microscopy to determine the IgM internalization (cell surface was stained by wheat germ agglutinin). The *insets* show a high magnification of the cells indicated by arrows. Scale bars, 10 μm (5 μm in the *insets*). Similar results were obtained in three different experiments. (**C**) Sorted T cells treated with BFM during incubation with IgMh1 or IgMm1 to inhibit lysosomal degradation and subjected to trypsin digestion to remove surface IgM were analyzed, as described in (B). The *insets* show a high magnification of the cells indicated by arrows. Scale bars, 10 μm (5 μm in the *insets*). Similar results were obtained in three different experiments. (**D**) Sorted T cells were treated with BFM during incubation with IgMh1 to inhibit lysosomal degradation and analyzed by confocal microscopy to determine intracellular localization of IgM. Lysosomal compartments were stained by anti–LAMP-1 mAb. Scale bars, 5 μm. Similar results were obtained in three different experiments.

IgMh1 (Fig. 1C). Furthermore, internalized IgM rapidly reached lysosomal compartments, as identified by LAMP-1 staining (Fig. 1D).

Internalized IgM inhibits T cell activation and proliferation

We then assessed whether IgM binding and internalization had any effect on T cell proliferation. PBMCs from healthy donors were incubated with the different IgM formulations and stimulated by anti-CD3/anti-CD28 for 72 h at 37°C. As shown in Fig. 2A, none of the tested IgM induced proliferation of T cells. However, IgM from healthy individuals (IgMh1, IgMh2) and two myeloma IgM (IgMm2 and IgMm3) strongly inhibited the proliferation of stimulated T cells. In contrast, IgMm1, the sole formulation that was not internalized, had a significantly reduced capacity to inhibit T cell proliferation. To further investigate the different activities of IgMh1 and IgMm1, we compared their effects on T cells committed to proliferate. Thus, during incubation with IgMh1 or IgMm1, PBMCs were stimulated for 1–4 d with anti-CD3/anti-CD28–coated beads or with PHA to induce a nonspecific T cell proliferation. As shown in Fig. 2E, IgMh1 efficiently inhibited T cell proliferation induced by the two different stimuli, whereas IgMm1 did not. It is likely that purified IgM acted directly on T cells, both CD4 and CD8 positive, because similar results were obtained when sorted populations were used. Indeed, IgMh1 still inhibited T cell proliferation, whereas IgMm1 showed reduced inhibitory ability (Fig. 2B–D).

We also analyzed the activation state of T cells treated with anti-CD3/anti-CD28 stimulus by low-density gene expression arrays. As expected, T cell activation was only partially inhibited by IgMm1; in contrast, IgMh1 had a strong effect in downregulating the expression of many genes involved in the immune response (Table I), including the proinflammatory factors IL-1α, IL-6, IL-17, IFN-γ, and TNF, and the activating and costimulatory molecules IL-2Rα and CD28. Interestingly, IgMh1 also downregulated genes coding for the inhibitory CTLA-4 and the regulatory IL-10 factors, as well as for the Th2-polarizing cytokine IL-5, whereas the expression of the Th2-specific IL-13 was significantly increased.

The inhibitory effects of IgM on T cells depend on the N-sialylation of IgM

To determine whether the inhibitory activity of IgM on T cells could depend on intrinsic structural characteristics, we analyzed the different IgM formulations. Western blot analyses revealed high levels of J chain in polyclonal IgMh1 and IgMh2 and in monoclonal IgMm2, all inhibitory, whereas low levels of J chain were found in the poorly inhibitory IgMm1. However, low levels of J chain were also present in the inhibitory IgMm3 (Fig. 3C). We then hypothesized that the different inhibitory effects of IgM could depend on different glycosylation. The glycosylation pattern of the IgM formulations was determined by HILIC-UPLC-FLD. Fig. 4A shows that all the inhibitory IgM are rich in terminal sialic acid residues. In contrast, IgMm1 is completely nonsialylated. To confirm the potential role of terminal sialic acids in the immunomodulatory effect of IgM on T cells, we treated IgMh1 with neuraminidase, an enzyme that selectively cleaves sialic acid moieties, and confirmed the sugar removal by HILIC-UPLC-FLD (Fig. 4B). Clearly, enzymatic desialylation abrogated the internalization and the inhibitory activity of IgM (Fig. 3A, 3B). However, the neuraminidase treatment did not significantly affect J chain content or polymeric structure of IgM (Fig. 3C, 3D). Furthermore, we analyzed the inhibitory effect of N-sialylated glycoproteins other than IgM. As shown in Fig. 3A, neither fetuin nor transferrin, which are highly sialylated proteins, is able to inhibit T cell proliferation, suggesting that this is a prerogative of sialylated IgM.

Discussion

Five commercially available IgM formulations purified from the serum of human healthy donors (IgMh) or myeloma patients (IgMm) were employed in our experiments. Of these, only one

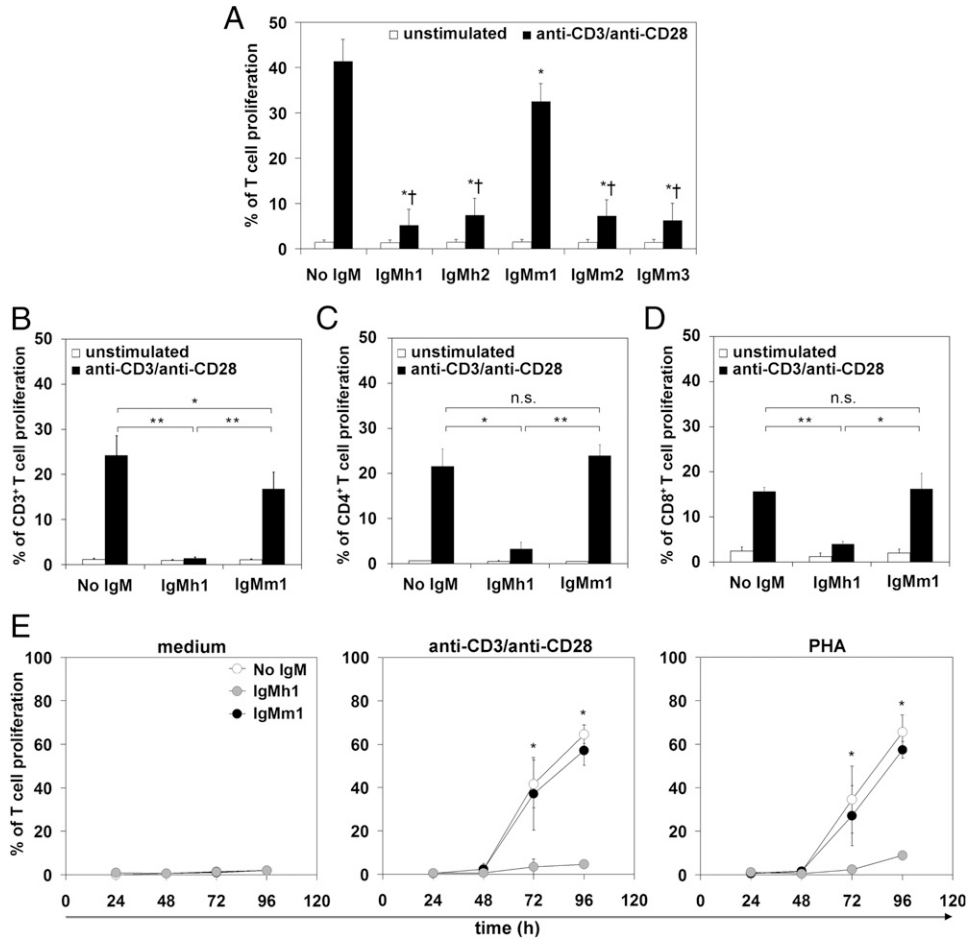

FIGURE 2. Effect of IgM on T cell proliferation. (**A**) CMFDA-labeled PBMCs incubated with different IgM formulations and stimulated with anti-CD3/anti-CD28–coated beads or complete medium for 72 h at 37˚C were stained with fluorescent Abs to CD3 and CD19. Gated living T cells were analyzed by FACS to determine T cell proliferation. Data represent the mean ± SEM ($n = 4$). *$p < 0.02$ versus stimulated T cells without IgM incubation, †$p < 0.05$ as compared with stimulated T cells incubated with IgMm1. (**B**) CMFDA-labeled sorted CD3-positive T cells were incubated with IgMh1 or IgMm1, stimulated with anti-CD3/anti-CD28–coated beads for 72 h at 37˚C, and analyzed by FACS to determine T cell proliferation. Data are represented as mean ± SD of four independent experiments. *$p < 0.05$, **$p < 0.01$, as determined by paired t test. (**C** and **D**) CMFDA-labeled sorted CD4-positive (C) or CD8-positive T cells (D) were treated as described in (B) and analyzed by FACS to determine T cell proliferation. Data are represented as mean ± SD of three independent experiments. *$p < 0.05$, **$p < 0.01$. n.s., not significant, as determined by paired t test. (**E**) CMFDA-labeled PBMCs incubated with IgMh1 or IgMm1 and stimulated with anti-CD3/anti-CD28–coated beads, PHA, or complete medium for 1–4 d at 37˚C were stained with fluorescent Abs to CD3 and CD19 and analyzed by FACS. Data represent the mean ± SEM ($n = 3$). *$p < 0.05$ cells incubated with IgMh1 versus cells incubated with complete medium.

myeloma IgM formulation (IgMm1) was detected on the surface of T cells after 24 h of incubation, and immunofluorescence analysis of sorted T cells showed that, whereas IgMm1 remained on the surface of T cells, IgMh1 bound T cells and became internalized. Furthermore, a fraction of IgMh1—but not of IgMm1—was found resistant to trypsin digestion, confirming the internalization of IgMh1. Therefore, the different binding of IgMh1 and IgMm1 to the surface of T cells appears to reflect failure of the latter to be internalized after binding to T cells. We then assessed whether IgM binding and internalization had any effect on proliferation of PBMCs from healthy donors in response to anti-CD3/anti-CD28 stimulation. Four IgM formulations strongly inhibited the proliferation of stimulated T cells. On the contrary, IgMm1, the formulation that was not internalized, had a significantly reduced capacity to inhibit T cell proliferation compared with the other IgM formulations. A similar inhibitory effect was observed when sorted T cells were incubated with IgM during an anti-CD3/anti-CD28 stimulation, suggesting that IgM acts directly on T lymphocytes, both CD4 and CD8 positive. Furthermore, as expected, IgMm1 was not efficient in inhibiting T cell activation, whereas IgMh1 induced a strong downmodulation of the expression of many proinflammatory genes. Interestingly, IgMh1 also downregulated genes coding for the inhibitory CTLA-4 and the regulatory IL-10 factors, suggesting that IgMh1 might induce an anergic state, rather than a regulatory phenotype, in stimulated T cells. Altogether, these findings suggest that the inhibitory effect of IgM is strongly associated with its internalization by T cells. We therefore asked what mechanisms are responsible for the internalization and the subsequent inhibitory activity of IgM on T cells. Some IgM might inhibit T cell activation and chemotaxis by targeting coreceptors and chemotactic receptors, such as CD3, CD4, CXCR4, and CCR5, or other molecules present on the surface of T cells, such as lipids or glycoproteins (12, 17–19). However, we show in this study that IgMh1 inhibited T cell proliferation induced also by nonspecific mitogenic stimulation with PHA. Furthermore, in our system, both polyclonal (IgMh1 and IgMh2) and monoclonal (IgMm2 and IgMm3) formulations had inhibitory effects, whereas monoclonal IgMm1 failed to inhibit T cell responses. We thus hypothesized that the different properties may be due to structural characteristics of IgM, such as

Table I. Gene expression levels

Gene	IgMh1 (RQ ± SD)[a]	Sig.[b]	IgMm1 (RQ ± SD)[a]	Sig.[b]	Gene	IgMh1 (RQ ± SD)[a]	Sig.[b]	IgMm1 (RQ ± SD)[a]	Sig.[b]
IL1A	0.1 ± 0.0	0.001	0.5 ± 0.1	NS	CD68	0.3 ± 0.2	0.009	0.7 ± 0.3	NS
IL5	0.4 ± 0.2	0.022	0.9 ± 0.7	NS	CTLA4	0.1 ± 0.1	<0.001	0.6 ± 0.2	0.017
IL6	0.2 ± 0.1	<0.001	0.5 ± 0.2	0.002	TBX21	0.4 ± 0.2	0.001	0.7 ± 0.2	NS
IL8	0.1 ± 0.1	<0.001	1.0 ± 0.5	NS	BCL2	0.3 ± 0.2	0.003	0.7 ± 0.3	NS
IL9	0.0 ± 0.0	<0.001	0.5 ± 0.1	0.002	BAX	0.5 ± 0.1	0.001	0.9 ± 0.0	NS
IL10	0.1 ± 0.1	<0.001	0.6 ± 0.3	NS	ICAM1	0.4 ± 0.1	<0.001	0.7 ± 0.1	0.010
IL13	3.0 ± 1.8	0.002	0.7 ± 0.3	NS	HMOX1	0.4 ± 0.2	0.014	0.9 ± 0.3	NS
IL17	0.1 ± 0.0	<0.001	0.7 ± 0.2	NS	IFNG	0.3 ± 0.1	<0.001	1.0 ± 0.2	NS
CCL3	0.2 ± 0.2	0.002	0.7 ± 0.3	NS	PRF1	0.5 ± 0.1	<0.001	1.1 ± 0.1	NS
CCL5	0.2 ± 0.1	<0.001	0.5 ± 0.2	NS	GZMB	0.1 ± 0.0	<0.001	1.0 ± 0.1	NS
STAT3	0.5 ± 0.2	0.002	0.6 ± 0.2	0.009	FASLG	0.2 ± 0.1	0.001	0.6 ± 0.3	NS
CD8A	0.3 ± 0.2	0.001	0.8 ± 0.3	NS	TNF	0.4 ± 0.1	<0.001	0.7 ± 0.2	NS
IL2RA	0.3 ± 0.2	0.001	0.6 ± 0.2	NS	LTA	0.3 ± 0.1	<0.001	0.8 ± 0.3	NS
CD28	0.3 ± 0.1	<0.001	0.7 ± 0.2	NS	VEGF	0.8 ± 0.5	NS	0.5 ± 0.1	0.018
PTPRC	0.4 ± 0.2	0.008	0.8 ± 0.4	NS					

[a]Sorted T cells stimulated by anti-CD3/anti-CD28 during incubation with IgMh1 or IgMm1 compared with T cells stimulated by anti-CD3/anti-CD28 without IgM incubation (control samples). Gene expression values are expressed as relative quantity (RQ) ± SD compared with control samples (RQ = 1; $n = 4$).

[b]Significant differences were calculated between T cells stimulated during incubation with IgMh1 or IgMm1 and control samples. The table reports only significantly different genes (ANOVA, $p < 0.05$).

Sig., significance.

the presence of J chains, shown before to be essential for transcytosis (20), and the state of polymerization (2, 21). Western blot analyses revealed high levels of J chain in polyclonal IgMh1 and IgMh2 and in monoclonal IgMm2, all inhibitory, whereas low levels of J chain were found in the poorly inhibitory IgMm1, but also in the inhibitory IgMm3, suggesting that the effect of IgM on T cells may not be dependent on J chain content. We then hypothesized that the different inhibitory effects of IgM could depend on different glycosylation. Human μ (heavy) chain presents five N-linked glycosylation sites, located at Asn^{171}, Asn^{332}, Asn^{395}, Asn^{402}, and Asn^{563}; the latter four reside in the fragment crystallizable (Fc). The N-linked glycans are prevalently composed of a core of biantennary polysaccharides containing two core GlcNAc residues and variable numbers of mannose residues. Further modifications can be observed with a core fucose linked to the inner GlcNAc residue, or terminal galactose and sialic acid residues variably present on the antennae. The J chain has a single N-linked glycosylation site, whereas light chains have none. Although binding of IgM to Ag modifies the exposure of glycans (22), little is known to date on the effects of glycosylation on IgM-binding activity. The glycosylation pattern of the IgM formulations was determined by HILIC-UPLC-FLD. All the inhibitory IgM resulted rich in terminal sialic acid residues. In contrast, the poorly inhibitory IgMm1 is completely nonsialylated. Furthermore, when we treated IgMh1 with neuraminidase, an enzyme that selectively cleaves sialic acid residues, we observed that enzymatic desialylation abrogated the internalization and the inhibitory activity of IgM, without affecting J chain content or polymeric structure of IgM. Therefore, sialylation is necessary for the internalization and the inhibitory effects of IgM on T cells. Of note, the immunomodulatory effect is specific of sialylated IgM, because other glycoproteins rich in N-linked sialic acids, such as fetuin and transferrin, did not inhibit T cell proliferation. Our findings support the concept that extensive sialylation of Igs stimulates immune suppression, as already demonstrated for the anti-inflammatory effects of i.v. γ globulin (IVIg) used to treat specific autoimmune and inflammatory diseases (13, 23, 24). Data from several mouse models of autoimmune diseases such as in-

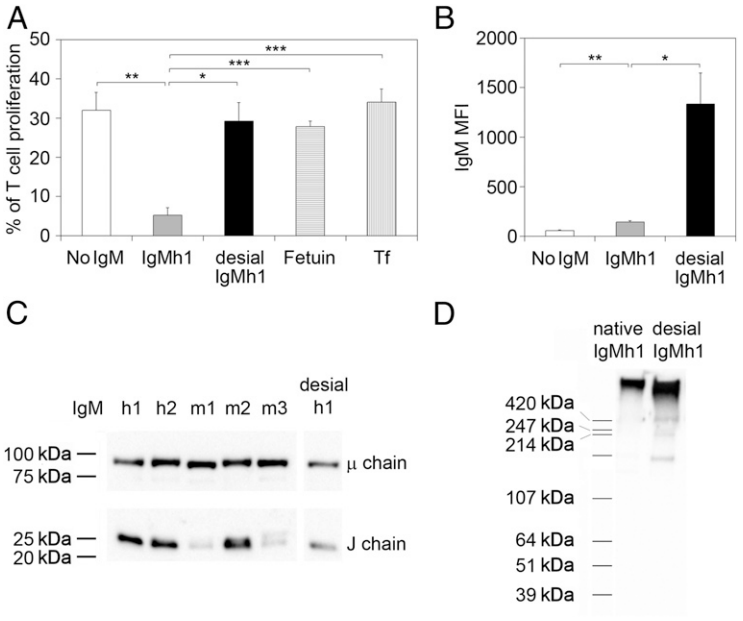

FIGURE 3. Uptake and immunomodulatory effects of IgM on T cells require sialic acid. (**A**) CMFDA-labeled PBMCs incubated with native or desialylated IgMh1, fetuin, and transferrin, or complete medium, and stimulated with anti-CD3/anti-CD28–coated beads for 72 h at 37°C, were stained with fluorescent Abs to CD3 and CD19. Gated living T cells were analyzed by FACS to determine T cell proliferation. Data represent the mean ± SD ($n = 3$). *$p < 0.05$, **$p < 0.02$, ***$p < 0.01$, as determined by paired t test. (**B**) PBMCs incubated with native or desialylated IgMh1 were stained with fluorescent Abs to CD3, CD19, and IgM, and the IgM mean fluorescence intensity was analyzed by FACS on gated living T cells. Data represent the mean ± SD ($n = 3$). *$p < 0.05$, **$p < 0.02$. (**C**) Different IgM in native or desialylated form were separated onto a reducing 10% SDS-PAGE gel, and μ and J chain expression was detected. (**D**) Native or desialylated IgMh1 were separated onto a nonreducing 4–15% gradient SDS-PAGE gel, and blots were decorated with anti–μ-chain Ab.

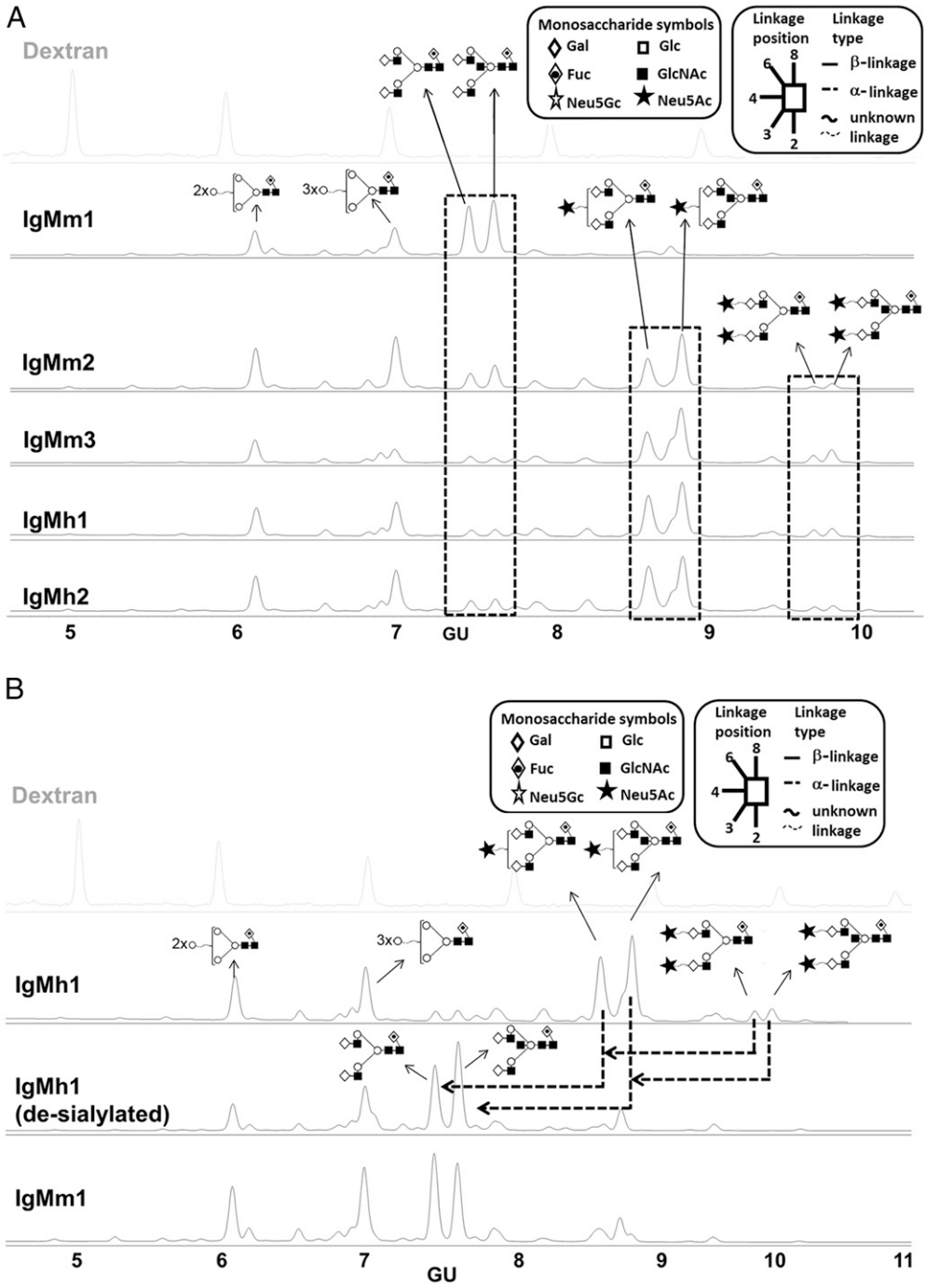

FIGURE 4. Glycan analyses. HILIC-FLD-UPLC chromatograms of N-linked glycans released from IgM. Glycans are represented using the Oxford symbol nomenclature (16). (**A**) Glycan profiles of commercial IgM. Arrows indicate the structures of the glycan peaks. (**B**) Glycan analysis of IgMh1 before and after enzymatic desialylation, compared with IgMm1. Dashed arrows depict the conversion of mono- and bis-sialylated IgM to the asialylated IgM. Fuc, fucose; Gal, galactose; Glc, glucosamine; GlcNAc, N-acetylglucosamine; GU, glucose units; Neu5Ac, sialic acid.

duced K/B×N arthritis and immunothrombocytopenia indicate that the preventive as well as therapeutic anti-inflammatory effects induced by IVIg administration depend on sialic acid terminal residues (13, 25–27). Indeed, IgG rich in sialic acid residues has shown a reduced ability to bind to activating FcγRs (25) and an acquired affinity for mouse-specific ICAM3-grabbing nonintegrin-related 1 (SIGNR1) and human dendritic cell SIGN (DC-SIGN) (26), as well as a capability to induce the expression of inhibitory FcγRIIB on innate immune cells (25, 27). In addition to these widely described mechanisms, a novel C-type lectin dendritic cell immunoreceptor was recently described to mediate the induction of regulatory T cells in an allergic airways disease model following IVIg infusion (28). Moreover, IVIg treatment was shown to be effective in inducing an anergic state in human B cells (29). All of these effects were dependent on the sialic acid content of IVIg, showing that the sialylation of Igs exerts inhibitory activity on both innate and adaptive immune responses.

In our system, we observed that IgM acted directly on T cells. Since 1975, T cells bearing FcR for IgM or IgG have been described (30, 31). These receptors have a rapid turnover on the cell membrane and can be modulated by the binding of IgG– or IgM–Ag complexes (FcμR in particular), whereas their identity has not

been determined (32). To date, three FcμR have been described, as follows: a Fcα/μR, a polymeric IgR (pIgR), and the simply called FcμR (33). Fcα/μR and pIgR bind both IgM and IgA (pIgR requires J chain for binding Abs) and are expressed in nonhematopoietic tissues and on B cells and macrophages (Fcα/μR) or on the basolateral surface of mucous epithelium and duct of excretory glands (pIgR). The FcμR is the only FcR constitutively expressed on both CD4-positive and CD8-positive T cells that selectively binds IgM with very high affinity, and is also expressed on B lymphocytes (33–36). It binds pentameric IgM 100 times more strongly than monomeric IgM (34) and is rapidly internalized upon IgM binding (35). Therefore, we can hypothesize that a FcμR binds sialylated IgM and its internalization may activate inhibitory pathways. On the contrary, desialylated IgM may be recognized by the same FcμR, and their altered conformation may prevent internalization and the subsequent inhibitory effects on T cells. However, we cannot exclude the possibility that sialylated and desialylated IgM are recognized by different IgM receptors. Interestingly, we observed that internalized IgM was rapidly shuttled to lysosomal compartments, as described by Vire et al. (35), upon FcμR binding. Further studies with blocking Abs directed against FcμR or with T cells silenced for FcμR may help to elucidate potential interactions between sialylated and nonsialylated IgM and FcμR.

In summary, our results indicate that the sialylation state determines the ability of IgM to be internalized by T cells and to inhibit their activation, showing for the first time, to the best of our knowledge, a tight structure–function relationship of IgM glycans. It remains to be seen which receptors mediate binding and internalization, and whether and which pathophysiological conditions influence the activity of the intracellular sialyltransferase.

Acknowledgments

We thank Maria Pia Rastaldi, Manuela Rosado, and Rita Carsetti for critical revision and discussion and Anna Taranta, Giusi Prencipe, Francesco Bellomo, and Laura Rega for help in experimental issues.

Disclosures

The authors have no financial conflicts of interest.

References

1. Ehrenstein, M. R., and C. A. Notley. 2010. The importance of natural IgM: scavenger, protector and regulator. *Nat. Rev. Immunol.* 10: 778–786.
2. Randall, T. D., J. W. Brewer, and R. B. Corley. 1992. Direct evidence that J chain regulates the polymeric structure of IgM in antibody-secreting B cells. *J. Biol. Chem.* 267: 18002–18007.
3. Müller, R., M. A. Gräwert, T. Kern, T. Madl, J. Peschek, M. Sattler, M. Groll, and J. Buchner. 2013. High-resolution structures of the IgM Fc domains reveal principles of its hexamer formation. *Proc. Natl. Acad. Sci. USA* 110: 10183–10188.
4. Kaveri, S. V., G. J. Silverman, and J. Bayry. 2012. Natural IgM in immune equilibrium and harnessing their therapeutic potential. *J. Immunol.* 188: 939–945.
5. Dorsett, B., W. Cronin, V. Chuma, and H. L. Ioachim. 1985. Anti-lymphocyte antibodies in patients with the acquired immune deficiency syndrome. *Am. J. Med.* 78: 621–626.
6. Lobo, P. I. 1981. Nature of autolymphocytotoxins present in renal hemodialysis patients: their possible role in controlling alloantibody formation. *Transplantation* 32: 233–237.
7. Winfield, J. B., P. D. Fernsten, and J. K. Czyzyk. 1997. Anti-lymphocyte autoantibodies in systemic lupus erythematosus. *Trans. Am. Clin. Climatol. Assoc.* 108: 127–135.
8. Lobo, P. I., K. H. Schlegel, C. E. Spencer, M. D. Okusa, C. Chisholm, N. McHedlishvili, A. Park, C. Christ, and C. Burtner. 2008. Naturally occurring IgM anti-leukocyte autoantibodies (IgM-ALA) inhibit T cell activation and chemotaxis. *J. Immunol.* 180: 1780–1791.
9. Lobo, P. I., K. H. Schlegal, J. Vengal, M. D. Okusa, and H. Pei. 2010. Naturally occurring IgM anti-leukocyte autoantibodies inhibit T-cell activation and chemotaxis. *J. Clin. Immunol.* 30(Suppl. 1): S31–S36.
10. Lobo, P. I., A. Bajwa, K. H. Schlegel, J. Vengal, S. J. Lee, L. Huang, H. Ye, U. Deshmukh, T. Wang, H. Pei, and M. D. Okusa. 2012. Natural IgM anti-leukocyte autoantibodies attenuate excess inflammation mediated by innate and adaptive immune mechanisms involving Th-17. *J. Immunol.* 188: 1675–1685.
11. Chhabra, P., K. Schlegel, M. D. Okusa, P. I. Lobo, and K. L. Brayman. 2012. Naturally occurring immunoglobulin M (nIgM) autoantibodies prevent autoimmune diabetes and mitigate inflammation after transplantation. *Ann. Surg.* 256: 634–641.
12. Lobo, P. I., K. L. Brayman, and M. D. Okusa. 2014. Natural IgM anti-leucocyte autoantibodies (IgM-ALA) regulate inflammation induced by innate and adaptive immune mechanisms. *J. Clin. Immunol.* 34(Suppl. 1): S22–S29.
13. Schwab, I., and F. Nimmerjahn. 2013. Intravenous immunoglobulin therapy: how does IgG modulate the immune system? *Nat. Rev. Immunol.* 13: 176–189.
14. Livak, K. J., and T. D. Schmittgen. 2001. Analysis of relative gene expression data using real-time quantitative PCR and the 2(-Delta Delta C(T)) method. *Methods* 25: 402–408.
15. Stöckmann, H., B. Adamczyk, J. Hayes, and P. M. Rudd. 2013. Automated, high-throughput IgG-antibody glycoprofiling platform. *Anal. Chem.* 85: 8841–8849.
16. Harvey, D. J., A. H. Merry, L. Royle, M. P. Campbell, R. A. Dwek, and P. M. Rudd. 2009. Proposal for a standard system for drawing structural diagrams of N- and O-linked carbohydrates and related compounds. *Proteomics* 9: 3796–3801.
17. Silverman, G. J., J. Vas, and C. Grönwall. 2013. Protective autoantibodies in the rheumatic diseases: lessons for therapy. *Nat. Rev. Rheumatol.* 9: 291–300.
18. Wu, X., N. Okada, M. Iwamori, and H. Okada. 1996. IgM natural antibody against an asialo-oligosaccharide, gangliotetraose (Gg4), sensitizes HIV-I infected cells for cytolysis by homologous complement. *Int. Immunol.* 8: 153–158.
19. Mimura, T., P. Fernsten, M. Shaw, W. Jarjour, and J. B. Winfield. 1990. Glycoprotein specificity of cold-reactive IgM antilymphocyte autoantibodies in systemic lupus erythematosus. *Arthritis Rheum.* 33: 1226–1232.
20. Johansen, F. E., R. Braathen, and P. Brandtzaeg. 2001. The J chain is essential for polymeric Ig receptor-mediated epithelial transport of IgA. *J. Immunol.* 167: 5185–5192.
21. Petrušić, V., I. Zivković, M. Stojanović, I. Stojićević, E. Marinković, A. Inić-Kanada, and L. Dimitijević. 2011. Antigenic specificity and expression of a natural idiotope on human pentameric and hexameric IgM polymers. *Immunol. Res.* 51: 97–107.
22. Arnold, J. N., M. R. Wormald, D. M. Suter, C. M. Radcliffe, D. J. Harvey, R. A. Dwek, P. M. Rudd, and R. B. Sim. 2005. Human serum IgM glycosylation: identification of glycoforms that can bind to mannan-binding lectin. *J. Biol. Chem.* 280: 29080–29087.
23. Hess, C., A. Winkler, A. K. Lorenz, V. Holecska, V. Blanchard, S. Eiglmeier, A. L. Schoen, J. Bitterling, A. D. Stoehr, D. Petzold, et al. 2013. T cell-independent B cell activation induces immunosuppressive sialylated IgG antibodies. *J. Clin. Invest.* 123: 3788–3796.
24. Goulabchand, R., T. Vincent, F. Batteux, J. F. Eliaou, and P. Guilpain. 2014. Impact of autoantibody glycosylation in autoimmune diseases. *Autoimmun. Rev.* 13: 742–750.
25. Kaneko, Y., F. Nimmerjahn, and J. V. Ravetch. 2006. Anti-inflammatory activity of immunoglobulin G resulting from Fc sialylation. *Science* 313: 670–673.
26. Schwab, I., M. Biburger, G. Krönke, G. Schett, and F. Nimmerjahn. 2012. IVIg-mediated amelioration of ITP in mice is dependent on sialic acid and SIGNR1. *Eur. J. Immunol.* 42: 826–830.
27. Schwab, I., S. Mihai, M. Seeling, M. Kasperkiewicz, R. J. Ludwig, and F. Nimmerjahn. 2014. Broad requirement for terminal sialic acid residues and FcγRIIB for the preventive and therapeutic activity of intravenous immunoglobulins in vivo. *Eur. J. Immunol.* 44: 1444–1453.
28. Massoud, A. H., M. Yona, D. Xue, F. Chouiali, H. Alturaihi, A. Ablona, W. Mourad, C. A. Piccirillo, and B. D. Mazer. 2014. Dendritic cell immunoreceptor: a novel receptor for intravenous immunoglobulin mediates induction of regulatory T cells. *J. Allergy Clin. Immunol.* 133: 853-863.e5.
29. Seite, J. F., C. Goutsmedt, P. Youinou, J. O. Pers, and S. Hillion. 2014. Intravenous immunoglobulin induces a functional silencing program similar to anergy in human B cells. *J. Allergy Clin. Immunol.* 133: 181-188.e1-9.
30. Ferrarini, M., L. Moretta, R. Abrile, and M. L. Durante. 1975. Receptors for IgG molecules on human lymphocytes forming spontaneous rosettes with sheep red cells. *Eur. J. Immunol.* 5: 70–72.
31. Moretta, L., M. Ferrarini, M. L. Durante, and M. C. Mingari. 1975. Expression of a receptor for IgM by human T cells in vitro. *Eur. J. Immunol.* 5: 565–569.
32. Mingari, M. C., L. Moretta, A. Moretta, M. Ferrarini, and J. L. Preud'homme. 1978. Fc-receptors for IgG and IgM immunoglobulins on human T lymphocytes: mode of re-expression after proteolysis or interaction with immune complexes. *J. Immunol.* 121: 767–770.
33. Klimovich, V. B. 2011. IgM and its receptors: structural and functional aspects. *Biochemistry* 76: 534–549.
34. Kubagawa, H., S. Oka, Y. Kubagawa, I. Torii, E. Takayama, D. W. Kang, G. L. Gartland, L. F. Bertoli, H. Mori, H. Takatsu, et al. 2009. Identity of the elusive IgM Fc receptor (FcmuR) in humans. *J. Exp. Med.* 206: 2779–2793.
35. Vire, B., A. David, and A. Wiestner. 2011. TOSO, the Fcmicro receptor, is highly expressed on chronic lymphocytic leukemia B cells, internalizes upon IgM binding, shuttles to the lysosome, and is downregulated in response to TLR activation. *J. Immunol.* 187: 4040–4050.
36. Kubagawa, H., S. Oka, Y. Kubagawa, I. Torii, E. Takayama, D. W. Kang, D. Jones, N. Nishida, T. Miyawaki, L. F. Bertoli, et al. 2014. The long elusive IgM Fc receptor, FcμR. *J. Clin. Immunol.* 34(Suppl. 1): S35–S45.